Current Optics and Photonics
Vol. 1, No. 4, August 2017, pp. 278-283

ISSN: 2508-7266(Print) / ISSN: 2508-7274(Online)
DOI: https://doi.org/10.3807/COPP.2017.1.4.278

Response of Water Tetramer to Intense Femtosecond Laser Pulses

Zhiping Wang*, Xuefen Xu, Chaoyi Qian, Yanbiao Wang, and Xu Wang

Department of Fundamental Courses, Wuxi Institute of Technology, 214121 Wuxi, P. R. China

(Received October 12, 2016 : revised March 17, 2017 : accepted May 18, 2017)

We theoretically study the dynamics of water tetramer in intense femtosecond laser pulses with different frequencies. The simulations are carried out by incorporating the molecular dynamics method non-adiabatically into the time-dependent local-density approximation (TDLDA-MD). Three typical scenarios of water tetramer including the normal vibration with enlarged OH bonds, free OH bonds breaking and the pure Coulomb explosion are presented by investigating the electronic and ionic dynamics. The result indicates that the ionization is enhanced and the corresponding fragmentation effect as well as the damping of the dipole moment are found more notably when increasing the laser frequency especially when the frequency falls in the resonant region of the absorption spectra. The study of the level depletion reveals that the ratio of the emission amount from different levels can be controlled by changing the laser frequency referring to the Keldysh parameter.

Keywords : TDLDA, Ionization, Water tetramer
OCIS codes : (020.0020) Atomic and molecular physics; (140.0140) Lasers and laser optics; (320.2250) Femtosecond phenomena

I. INTRODUCTION

With the development of the laser technology, the interaction of intense ultrashort laser pulses with material has been explored many times both in experiment and theory [1-3]. Compared to atoms in intense fields, molecules exhibit versatile phenomena due to their additional degrees of freedom [4-6]. Water has attracted much attention with a variety of experimental and theoretical techniques due to its various physical states [7-9]. Water cluster is always used as a vehicle for better understanding how bulk properties of water arise from the isolated water molecule as the cluster size is increased. Recently, the experimental study of the photo-induced real time dynamics of a water cluster in intense sub-50 fs vacuum ultraviolet laser pulses has been performed and three relevant time scales are distinguished [10]. The rates of proton transfer along a hydrogen bond in a water cluster cation have been investigated by means of a direct ab initio molecular dynamics method [11]. In the present work, applying the time-dependent local-density approximation coupled with molecular dynamics method (TDLDA-MD) we explore the irradiation dynamics of water tetramer in intense femtosecond laser pulses with different laser frequencies. TDLDA-MD has become a full-fledged method to explore the real-time dynamics of multi-electron system under intense laser field [12-18]. Our aim is to investigate the irradiation effect on a water cluster under ultrashort laser pulses. The water tetramer owning the ring structure with S_4 symmetry is expected to behave rather differently from both the trimer and the pentamer [19]. The result presented here is in succession to our foregoing study [14, 18]. We expect that the present calculated results would help in better understanding of the process of photo-induced dynamics of water clusters in laser fields.

II. METHODS

In the TDLDA-MD framework [12], the degrees of the molecule are the wave functions of valence electrons and the coordinates of the ionic cores. For a water tetramer, it is composed of 32 valence electrons and 12 ions. A norm-

*Corresponding author: zpwang03247@163.com
Color versions of one or more of the figures in this paper are available online.

conserving pseudopotential including a local part and a non-local part is applied to describe the interaction between ions and electrons [20]. The time-dependent Kohn-Sham (TDKS) equation [21] for single-particle orbitals $\phi_j(r,t)$ is applied to describe the motion of valence electrons. An average-density self-interaction correction (ADSIC) [22] is used to put the single-particle energies at their correct values. Ions are treated as classical particles and the ionic motion of the water tetramer is described within standard molecular dynamics. The ground state wavefunctions are achieved through the damped gradient method [12] and the TDLDA equations are solved numerically on a grid 3D coordinate space. A constant time step $\Delta t = 0.000605$ fs is used for the evolution of electrons and ions. The absorbing boundary condition is applied to avoid periodic reflecting electrons [23]. The laser field is defined as $E_{las}(t) = E_0 f_{las}(t) \cos(\omega t)$, where E_0 and ω denote the maximum amplitude of electric field and the laser frequency. $f_{las}(t)$ is the pulse profile taking the form of $\cos^2$ and the Full Width Half Maximum (FWHM) is 8 fs. The number of escaped electrons is defined as $N_{esc}(t) = N(t=0) - \int_V \mathrm{d}^3 r \rho(\boldsymbol{r},t)$, where $\rho(\boldsymbol{r},t)$ denotes the electronic density within the finite volume V centered around ions. The ionization out of state j is defined as $n_{esc,j}(t) = \int_V \mathrm{d}^3 r \left|\phi_j(\boldsymbol{r},t)\right|^2 = \int_V \mathrm{d}^3 r \rho_j(\boldsymbol{r},t)$ and $\rho_j(\boldsymbol{r},t)$ is the single-particle Kohn-Sham density. The real-time evolution of the dipole moment is given by $D_i(t) = \int d^3 \boldsymbol{r} r_i \rho(\boldsymbol{r},t)$, with $i = x, y, z$. The optical absorption strength is the imaginary part of $\tilde{D}(\omega)$ which is obtained by Fourier transform the dipole momentum $D(t)$ [24].

III. RESULTS AND DISCUSSION

In the present study, the water tetramer is placed in a cuboid box with the size of $96 \times 96 \times 96$ spatial grid points with each mesh spacing of $0.412a_0$ to ensure a convergent calculation. The left panel in Fig. 1 shows the optimal configuration of the water tetramer owning the ring structure with S_4 symmetry, which is nearly planar structure.

In the water tetramer four water molecules act as both proton donors and acceptors. Thus, there are four hydrogen bonds in water tetramer which are O_1H_4, $O_{10}H_9$, O_5 H_{12} and O_7H_2. Moreover, there are eight OH bonds which could be classified into two categories, i.e. free OH bonds (O_1H_3, O_5H_6, O_7H_8 and $O_{10}H_{11}$) and bonded OH bonds (O_1H_2, O_5H_4, O_7H_9 and $O_{10}H_{12}$). Due to the degeneracy of spin up and spin down states, there are 16 occupied states. The right panel in Fig. 1 displays the calculated electronic density of the respective orbitals from the HOMO level and to the most deep occupied electronic level (the occupied single-particle state owning the lowest energy) in the *xy* plane. The red and gray circles represent the oxygen and hydrogen ions respectively. One can see that the electronic density distributes intensively around the water tetramer in the numerical box indicating that the computation space is large enough to launch the dynamic simulation.

We calculate the ionization potential I_p of the water tetramer. It corresponds to the energy of the last occupied electron state of the water tetramer. Table 1 compiles the ionization potential of the water tetramer obtained by different methods, together with experimental value. It is

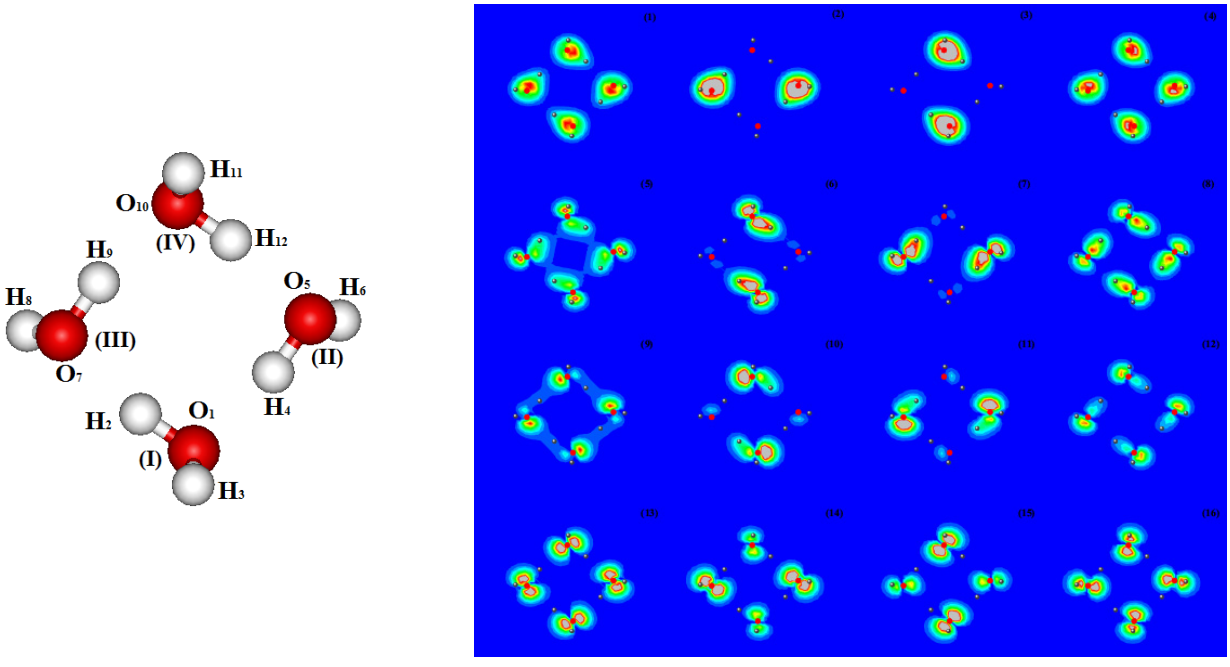

(a) (b)

FIG. 1. (a) optimal structure of water tetramer and the labeling of the atoms. (b) the contour plots of the electronic density of the respective molecular orbitals of water tetramer in the *xy* plane calculated by TDLDA-MD.

TABLE 1. The ionization potential (I_p , in eV) of water tetramer obtained by different methods, together with the corresponding experimental data available in literature

This Work	Experimental [25]	MP2/6-31++G** [26]	CCSD/aug-cc-pVDZ [27]	MP2/6-311++G(d, p) [11]
10.37	10.94	12.10	11.93	12.2

shown that our calculated ionization potential accords well with the experimental value, indicating the accuracy of our simulation.

It is known that the irradiation dynamics can be implemented by adjusting pulse parameters such as frequency, pulse number, intensity and phase [15, 28]. We explore the non-adiabatic dynamics of the water tetramer in different laser fields by varying the laser frequencies, which are $\omega =$ 1.55 eV, 5.44 eV and 13.0 eV, respectively. It should be noted that in the former two cases the laser frequencies are far below all eigenmodes in the optical absorption spectra of the water tetramer, while $\omega = 13.0$ eV falls into the continuum region and is above the ionization potential. In all cases the laser polarization is along the x axis. The Keldysh parameter [29] takes the form of $\gamma = \sqrt{I_p/2U_p}$, where I_p and U_p are the ionization potential and the ponderomotive energy respectively. In these three cases $\gamma = 0.54$, 1.89 and 4.52 respectively. It is known that the Keldysh parameter separates the multiphotonic domain ($\gamma > 1$) and the tunnelling regime ($\gamma < 1$). Therefore, the first case belongs to the tunnelling ionization and the latter two cases pertain to the multiphotonic ionization. The laser pulse is turned off at 16 fs. In order to observe the dynamics of the water tetramer during the relaxation time, we track the calculations until 35 fs in the case of $\omega = 1.55$ eV and until 55 fs in the cases of $\omega = 5.44$ eV and 13.0 eV.

Figure 2 shows the time evolutions of the ionization N_{esc} of the water tetramer in three different laser fields by varying laser frequencies. Figure 3 gives the snapshots of the evolving process of the water tetramer in three cases as shown in Fig. 2. In the first case of $\omega = 1.55$ eV, one can see that the ionization increases quickly from about 4 fs to 12 fs. There are about two electrons emitted when the laser pulse is switched off at 16 fs and no more electrons are emitted in the remaining time. Thus, the water tetramer keeps on the gentle stretching vibration coupled with the rotation mode as shown in Fig. 3(a). In addition, the calculated average stretching frequency of OH bonds in the present case is about 3243 cm^{-1}. Compared with the experimental values of 3714 cm^{-1} and 3416 cm^{-1} corresponding to the free OH stretching frequency and the bonded OH stretching frequency [30], the present average stretching frequency is red shifted due to the fact that the OH bond lengths are enlarged as a result of the ionization.

In the second situation of $\omega = 5.44$ eV as shown in Fig. 2, there are about 3.7 electrons emitted rapidly from about 4 fs to 16 fs, making the water tetramer unstable. Thus, one can see from Fig. 3(b) the breaks of free OH bonds O_5H_6 and O_7H_8 indicating the stronger response of free OH bonds than that of bonded OH bonds. Although the ionization is almost saturated after the laser pulse is turned off, there are about 0.4 electrons emitted additionally from 40 fs to 48 fs (see the red dashed line in Fig. 2). This is because the hydrogen ions (H_6 and H_8) carrying the electrons move toward the boundary of the numerical box

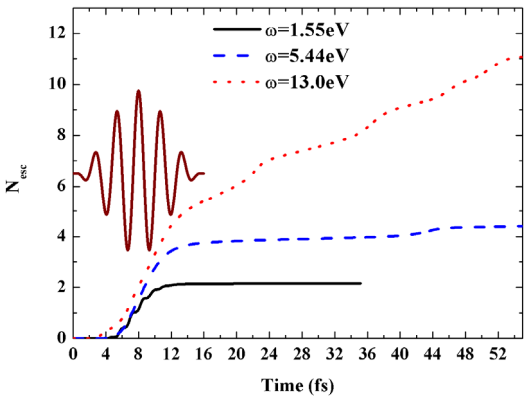

FIG. 2. Time evolutions of the number of emitted electrons N_{esc} of the water tetramer irradiated in laser pulses by varying the laser frequency as indicated. The applied $\cos^2$ pulse of FWHM = 8 fs and $\omega = 1.55$ eV is plotted.

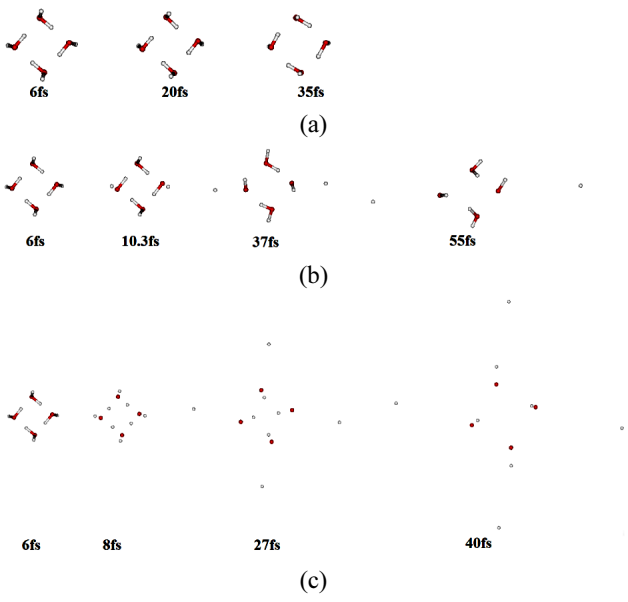

FIG. 3. Snapshots of the evolving process of the water tetramer in three cases as shown in Fig. 2: (a) $\omega = 1.55$ eV; (b) $\omega = 5.44$ eV; (c) $\omega = 13.0$ eV.

(as shown in Fig. 3(b)). Furthermore, it can be seen in Fig. 3(b) that after the breaks of two free OH bonds, the remaining parts keep on vibrating and rotating.

For the third case of $\omega = 13.0$ eV, it can be seen from Fig. 2 that the ionization increases rapidly from about 2 fs and almost five electrons are emitted directly until $t = 16$ fs leaving a highly excited water tetramer which then experiences Coulomb explosion. The snapshots in Fig. 3(c) show that the Coulomb explosion results in fast breaking of all OH bonds. Furthermore, each escaping hydrogen ion carries away the surrounding electron cloud leading to the continuous electron emission during the relaxation time.

In general, it can be seen in Fig. 2 that in the respective cases the ionization takes place predominantly in a time slot of about 8 fs around the peak of the laser pulse. The ionization is enhanced and the corresponding fragmentation effect is found more notably when increasing the laser frequency especially for the frequency falling in the resonant region of the absorption spectra. This pattern is similar to that found in the metal cluster and water molecule subjected to laser pulses [12, 17]. While it is different from the reaction of fullerene C_{60} in the laser pulse [31]. For C_{60}, it is found that the fragmentation effect is greater at low laser frequency rather than at the resonant frequency.

Figure 4 exhibits the time evolutions of the dipole moment of the water tetramer in the x direction in three cases. In the first case as shown in Fig. 4(a), the associated dipole signal in the x direction closely follows the laser profile. It attains an appreciable amplitude but fades away as soon as the laser pulse is turned off and keeps on slight oscillation in the relaxation time. This pattern is similar to the response of the water monomer and the metal cluster irradiated in the laser field with the frequency far below the resonant region [17, 23].

For the case of $\omega = 5.44$ eV, Fig. 4(b) exhibits clearly that from 0 fs to 8 fs the profile of the dipole moment is similar to that of the laser pulse, while then the dipole response shows the damping on account of the quick ionization shown in the red dashed line in Fig. 3. After switching off the laser pulse, because of the higher excitation than in the first case the dipole signal holds on to the stronger vibration than that in the first case.

In the case of $\omega = 13.0$ eV, the behavior of the dipole signal shown in Fig. 4(c) is quite different. It follows the laser amplitude from 0 fs to 6 fs, while then undergoes a much stronger damping in the course of time. This is mainly due to the high energetic excitation resulting in the rapid electron emission. Even when the pulse is turned off, because of the continuous electron emission and the ionic motion relating to the breaks of the OH bonds in the relaxation time, the amplitude of dipole signal fails and the dipole signal keeps on the much stronger oscillation than that in the former two cases.

In short, Fig. 4 exhibits visually how the electronic features of the water tetramer are dynamically influenced by the irradiation of laser pulses.

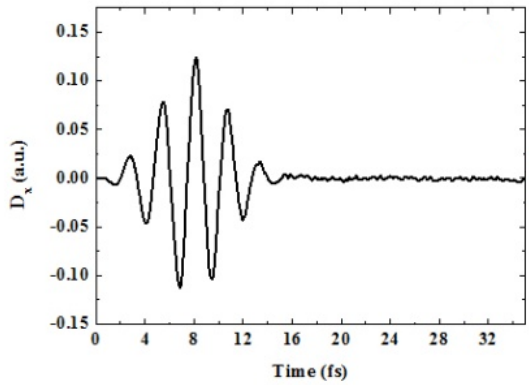

(a)

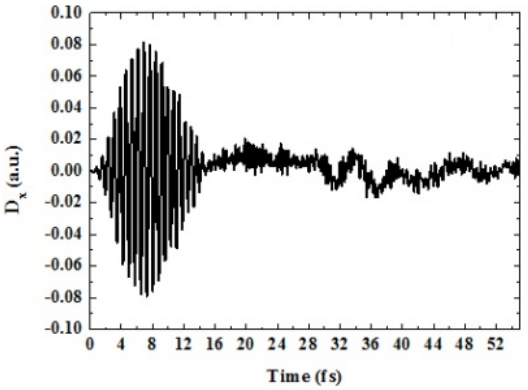

(b)

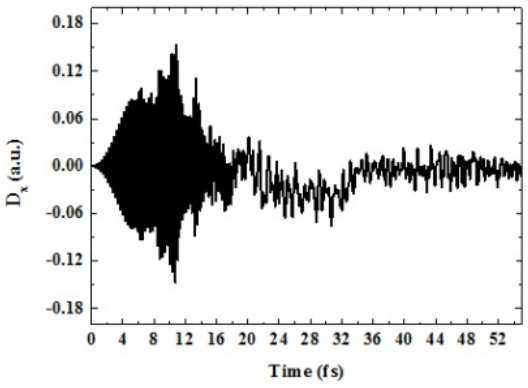

(c)

FIG. 4. Time evolutions of the dipole moment of the water tetramer in the x direction in three cases as shown in Fig. 2: (a) $\omega = 1.55$ eV; (b) $\omega = 5.44$ eV; (c) $\omega = 13.0$ eV.

Figure 5 shows the stationary single-electron spectrum with the amount of depletion of each occupied single-particle state. The positions at the y-axis stand for the 16 Kohn-Sham energies of the occupied single-particle states visualized in Fig. 1. The lowest position of -28.07 eV and the highest position of -10.37 eV represent the most deep occupied level and the HOMO level respectively. The length of the horizontal bar denotes the final depletion from each occupied single-particle state, i.e. the ionization from the respective single-particle state. As there are 16

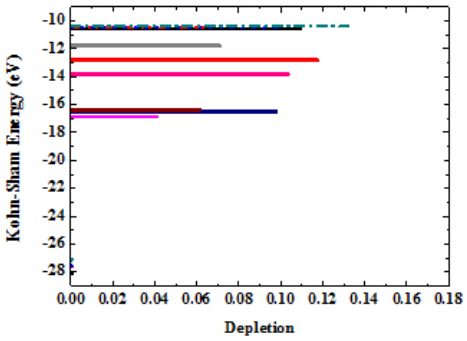

(a)

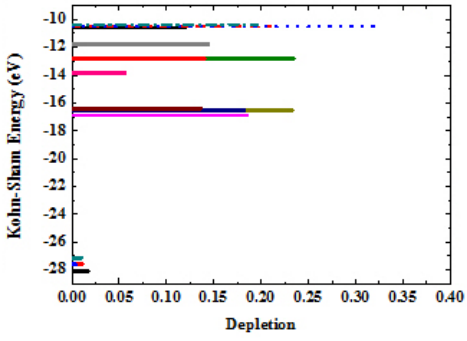

(b)

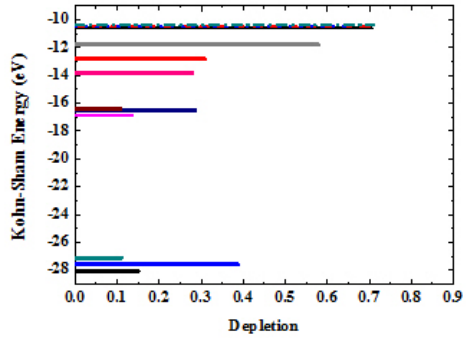

(c)

FIG. 5. Level depletion of water tetramer for the same cases as in Fig. 2.

single-particle states and some of states are degenerate with different values of m (three 1d states and two 1p states, and so on), the lines in Fig. 5 are plotted in different colors and types. It can be seen in Fig. 5(a) that in the case of $\omega = 1.55$ eV, i.e. in the tunnelling ionization case, all levels except the deepest occupied electronic levels contribute the emission equivalently. For the multiphotonic ionization cases as shown in Figs. 5(b) and 5(c), emission comes from all levels even the deepest occupied levels and the HOMO level contributes the most. Furthermore, one can also see in Fig. 5(c) that the emission from the deepest occupied levels are comparable with that from other states lower than the HOMO level. This can be traced back to the fact that the laser frequency above I_p is high enough to remove electrons from all states.

IV. CONCLUSION

In summary, applying the TDLDA-MD approach, we simulate the non-adiabatic dynamics of the water tetramer induced by intense laser pulses. We especially focus on the influence of the laser frequency on the electronic and ionic reactions of the water tetramer subject to the laser fields. Three laser frequencies are considered, i.e. $\omega = 1.55$ eV (far below the resonant region), $\omega = 5.44$ eV (below the resonant region) and $\omega = 13.0$ eV (in the resonant region and above the I_p). Three typical reaction channels, which are normal vibration with enlarged OH bonds, free OH bonds breaking and the pure Coulomb explosion are visually presented respectively. The study shows that the ionization is enhanced and the corresponding fragmentation effect as well as the damping of the dipole moment are found more notably when increasing the laser frequency especially for the frequency falling in the resonant region of the absorption spectra. The study of the level depletion reveals that in the tunnelling ionization case all levels except the deepest occupied electronic levels contribute the emission equivalently while in the multiphotonic ionization case the emission from the HOMO level is more than that from other states. In addition, the emission ratio from the deepest occupied levels is enhanced when the laser frequency is higher than the ionization potential. Our study illustrates that the various irradiation dynamics of the water tetramer can be realized by controlling the laser frequency. We hope the results will help the further experimental study.

ACKNOWLEDGMENT

This study was supported by the Natural Science Foundation of Jiangsu Province under Grants Nos. BK20160199, BK20150118 and 16KJB140024, by the Science Foundation of Wuxi Institute of Technology under Grant No. 3115006931.

REFERENCES

1. K. Yamanouchi, "The next frontier," Sci. **295**, 1659-1660 (2002).
2. M. Protopaps, C. H. Keitel, and P. I. Knight, "Atomic physics with super-high intensity lasers," Rep. Prog. Phys. **60**, 389-486 (1997).
3. S. I. Chu and D. A. Telnov, "Beyond the Floquet theorem: generalized Floquet formalisms and quasienergy methods for atomic and molecular multiphoton processes in intense laser fields," Phys. Rep. **390**, 1-131 (2004).
4. B. Friedrich and D. Herschbach, "Alignment and trapping of molecules in intense laser fields," Phys. Rev. Lett. **74**, 4623-4626 (1995).
5. L. Quaglia and C. Cornaggia, "Experimental evidence of excited multicharged atomic fragments coming from laser-induced coulomb explosion of molecules," Phys. Rev. Lett.

84, 4565-4568 (2000).
6. T. Zuo, S. Chelkowski, and A. D. Bandrauk, "Ionization rates of H_2^+ in an intense laser field by numerical integration of the time-dependent Schrödinger equation," Phys. Rev. A. **46**, R5342-R5345 (1992).
7. J. D. Smith, C. D. Cappa, K. R. Wilson, B. M. Messer, R. C. Cohen, and R. J. Saykally, "Energetics of hydrogen bond network rearrangements in liquid water," Sci. **306**, 851-853 (2004).
8. K. Liu, J. D. Cruzan, and R. J. Saykally, "Water clusters," Sci. **271**, 929-933 (1996).
9. R. Bukowski, K. Szalewicz, G. C. Groenenboon, and A. van der Avoird, "Predictions of the properties of water from first principles," Sci. **315**, 1249-1252 (2007).
10. H. T. Liu, J. P. Müller, M. Beutler, M. Ghotbi, F. Noack, W. Radloff, N. Zhavoronkov, C. P. Schulz, and I. V. Hertel, "Ultrafast photo-excitation dynamics in isolated, neutral water clusters," J. Chem. Phys. **134**, 094305(1-10) (2011).
11. H. Tachikawa and T. Takada, "Proton transfer rates in ionized water clusters $(H_2O)_2$ (n=2-4)," RSC Adv. **5**, 6945-6953 (2015).
12. F. Calvayrac, P.-G. Reinhard, E. Suraud, and C. A. Ullrich, "Nonlinear electron dynamics in metal clusters," Phys. Rep. **337**, 493-578 (2000).
13. Th. Fennel, K.-H. Meiwes-Broer, J. Tiggesbáumker, P.-G. Reinhard, P. M. Dinh, and E. Suraud, "Laser-driven nonlinear cluster dynamics," Rev. Mod. Phys. **82**, 1793-1842 (2010).
14. Z. P. Wang, P. M. Dinh, P.-G. Reinhard, E. Suraud, and F. S. Zhang, "Nonadiabatic effects in the irradiation of ethylene," Inter. J. Quanm. Chem. **111**, 480-486 (2011).
15. Y. L. Jiao, F. Wang, X. H. Hong, W. Y. Su, Q. H. Chen, and F. S. Zhang, "Electron dynamics in CaB_6 induced by one- and two-color femtosecond laser," Phys. Lett. A **377**, 823-827 (2013).
16. U. F. Ndongmouo-Taffoti, P. M. Dinh, P.-G. Reinhard, E. Suraud, and Z. P. Wang, "Exploration of dynamical regimes of irradiated small protonated water clusters," Eur. Phys. J. D **58**, 131-136 (2010).
17. Z. P. Wang, Y. M. Wu, X. M. Zhang, and C. Lu, "TDDFT study of excitation of water molecules with short laser pulses," Chin. Phys. B **22**, 073301(1-5) (2013).
18. Z. P. Wang, P. M. Dinh, P.-G. Reinhard, and E. Suraud, "Ultrafast nonadiabatic dynamics of water dimer in femtosecond laser pulses," Laser Phys. **24**, 106004(1-7) (2014).
19. D. J. Wales, T. R. Walsh, "Theoretical study of the water tetramer," J. Chem. Phys. **106**, 7193-7207 (1997).
20. S. Goedecker, M. Teter, and J. Hutter, "Separable dual-space Gaussian pseudopotentials," Phys. Rev. B **54**, 1703-1710 (1996).
21. E. K. U. Gross and W. Kohn, "Time-dependent density-functional theory," Adv. Quant. Chem. **21**, 255-291 (1990).
22. C. Legrand, E. Suraud, and P.-G. Reinhard, "Comparison of self-interaction-corrections for metal clusters," J. Phys. B **35**, 1115-1128 (2002).
23. C. A. Ullrich, "Time-dependent Kohn-Sham approach to multiple ionization," J. Mol. Struct. (THEOCHEM) **501-502**, 315-325 (2000) .
24. F. Calvayrac, P.-G. Reinhard, and E. Suraud, "Spectral signals from electronic dynamics in sodium clusters," Ann. Phys. (NY) **255**, 125-162 (1997).
25. L. Belau, K. R. Wilson, S. R. Leone, and M. Ahmed, "Vacuum Ultraviolet (VUV) photoionization of small water clusters," J. Phys. Chem. A **111**, 10075-10083 (2007).
26. P. A. Pieniazek, J. VandeVondele, P. Jungwirth, A. I. Krylov, and S. E. Bradforth, "Electronic structure of the water dimer cation," J. Phys. Chem. A **112**, 6159-6170 (2008).
27. S. M. Javier, M. Manuela, and R. S. Daniel, "Ab initio determination of the ionization potentials of water clusters $(H_2O)_n$ (n=2-6)," J. Chem. Phys. **136**, 244306 (2012).
28. C. Y. Zhang, J. W. Yao, C. Q. Li, Q. F. Dai, S. Lan, V. A. Trofimov, and T. M. Lysak, "Asymmetric femtosecond laser ablation of silicon surface governed by the evolution of surface nanostructures," Opt. Express **21**, 4439-4446 (2013).
29. L. V. Keldysh, "Ionization in the field of a strong electromagnetic wave," Sov. Phys. JETP **20**, 1307-1314 (1964).
30. F. Huisken, M. Kaloudis, and A. Kulcke, "Infrared spectroscopy of small size-selected water clusters," J. Chem. Phys. **104**, 17-25 (1996).
31. Z. Z. Lin and X. Chen, "Ultrafast dynamics and fragmentation of C_{60} in intense laser pulses," Phys. Lett. A **377**, 797-800 (2013).